IEEE Access
Multidisciplinary ⋮ Rapid Review ⋮ Open Access Journal

Received 1 June 2024, accepted 14 June 2024, date of publication 24 June 2024, date of current version 26 July 2024.

Digital Object Identifier 10.1109/ACCESS.2024.3418833

RESEARCH ARTICLE

A Novel Ultra-Compact Microstrip Coupler With Low Imbalance Magnitudes and Phases for Wireless Networks

SALAH I. YAHYA[1,2], (Senior Member, IEEE), FARID ZUBIR[3], (Member, IEEE), LEILA NOURI[4,5], ABBAS REZAEI[6], AND NOORLINDAWATY MD JIZAT[7], (Member, IEEE)

[1]Department of Communication and Computer Engineering, Cihan University-Erbil, Erbil 44001, Iraq
[2]Department of Software Engineering, Faculty of Engineering, Koya University, Koya KOY45, Iraq
[3]Wireless Communication Centre, Faculty of Electrical Engineering, Universiti Teknologi Malaysia, Johor Bahru, Johor 81310, Malaysia
[4]Institute of Research and Development, Duy Tan University, Da Nang 550000, Vietnam
[5]School of Engineering and Technology, Duy Tan University, Da Nang 550000, Vietnam
[6]Department of Electrical Engineering, Kermanshah University of Technology, Kermanshah 67146, Iran
[7]Faculty of Engineering, Multimedia University, Persiaran Multimedia, Cyberjaya, Selangor 63100, Malaysia

Corresponding authors: Farid Zubir (faridzubir@utm.my), Leila Nouri (leilanouri@duytan.edu.vn), and Noorlindawaty Md Jizat (noorlindawaty.jizat@mmu.edu.my)

This work was supported in part by the Higher Institution Centre of Excellence (HICOE), Ministry of Higher Education Malaysia, through the Wireless Communication Centre (WCC), Universiti Teknologi Malaysia, under Grant A.J091300.6800.09465 and Grant R.J090301.7823.4J610; and in part by the Faculty of Engineering, Multimedia University (MMU), Cyberjaya, Selangor, Malaysia.

ABSTRACT Based on stub loaded meandrous coupled lines, a novel microstrip coupler is designed, fabricated and measured for wireless applications. It is very compact with high performance. The size of this coupler is only 0.0028 λg^2, where it operates at 875 MHz. The values of S_{11}, S_{21}, S_{31} at the operating frequency are −24.97 dB, −3.058 dB and −3.033 dB respectively. Therefore, the insertion losses are very low and the magnitudes of S_{21} and S_{31} are well balanced. The phase imbalance at the operating frequency is 0.5°. From 790 MHz up to 1.18 GHz, S_{11} is better than −10 dB, the maximum phase imbalance is lower than 4.5° and the maximum magnitude imbalance is lower that ±0.5 dB. Therefore, it has 40% fractional bandwidth (FBW) that covers 0.79 GHz to 1.18 GHz. Its in-band isolation factor is better than −25 dB. The important advantages of this coupler compared to most of the previous designs is having a filtering frequency response and having flat passbands with a maximum group delay of 1 ns.

INDEX TERMS Wireless networks, microstrip, ultra-compact, coupler, suppressed harmonics, fractional bandwidth.

I. INTRODUCTION

Microstrip couplers specially filtering couplers are widely demanded by current wireless communication systems [1], [2], [3], [4], [5]. However, in most previous microstrip couplers the designers did not consider the filtering frequency response [6], [7], [8]. Some couplers that have filtering frequency response are not able to suppress any harmonics [9]. Having low losses, high isolation factor, balanced magnitude and phase are the other advantages of a well-designed coupler. Also, having low group delay in microstrip couplers is crucial for maintaining signal integrity and minimizing distortion in high-frequency communication systems. Three microstrip couplers with high losses, unsuppressed harmonics and unbalanced magnitudes and phases are introduced in [10], [11], and [12], while they have large implementation areas. A combination of microstrip and lumped elements is used to obtain a coupler with a phase imbalance less than 5° in [13]. However, using lumped element in addition to convert planar microstrip structure into three-dimensional lead to a complex fabrication process. An important parameter in performance evaluation of couplers is group delay, which is a measure of device phase distortion. In [14], a slot-coupling microstrip directional coupler is proposed by optimizing the

The associate editor coordinating the review of this manuscript and approving it for publication was Feng Wei.

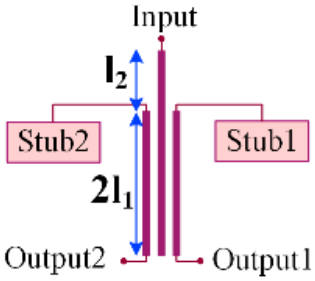

FIGURE 1. Basic semi-layout three-port structure.

generalized coupling slot on the printed circuit board (PCB). Some meandrous microstrip stubs are loaded inside a ring to obtain a branch line coupler with a filtering frequency response in [15]. However, it does not have a good frequency selectivity after its passband. In [16], a large size branch line coupler is designed using double-layered microstrip line.

In this study, a novel four-port structure will be proposed to solve the problems of the previous works in terms of large sizes, high losses, unbalanced magnitude and phase, harmonics, and high group delays. This coupler is well miniaturized with an ultra-compact size of 0.0028 λg^2, a fractional bandwidth (FBW) of 40% and a maximum group delay of 1 ns. The design process is started by introducing a basic semi-layout three-port structure. Then, it is analyzed mathematically to tune the operating frequency and miniaturization simultaneously. This basic structure includes two integrated bandpass filters (BPF). After that, the isolation port is coupled to the basic structure using a simple structure. The final dimensions of the proposed coupler are obtained using an optimization method. But the imprecise dimensions can be recognized by the presented mathematical and scientific analysis of the basic structure behavior. The size and performance of this coupler will be compared with the previous works to confirm its advantages. It will be shown that the measurement results of our fabricated coupler are in good agreement with the simulation results.

II. DESIGN AND ANALYSIS

To obtain a balanced 0° coupler, first we will design a three port bandpass structure. Then, the isolation port will be coupled to this structure. Fig. 1 shows the basic semi-layout three-port structure including common port (Input), direct and coupling ports (Outputs). In this structure, three thin transmission lines are coupled. The middle line is connected to the common port and the two other lines are loaded by shunt stubs.

The approximated *LC* circuits of the basic three-port structure and basic bandpass resonator are presented in Fig. 2(a) and Fig. 2(b) respectively. The proposed *LC* basic bandpass resonator shown in Fig. 2(b) is obtained based on the approximated *LC* circuits of the basic three-port structure, where we open Output 2. Hence, this open-end is replaced by a capacitor of C_O. The approximated equivalent of three

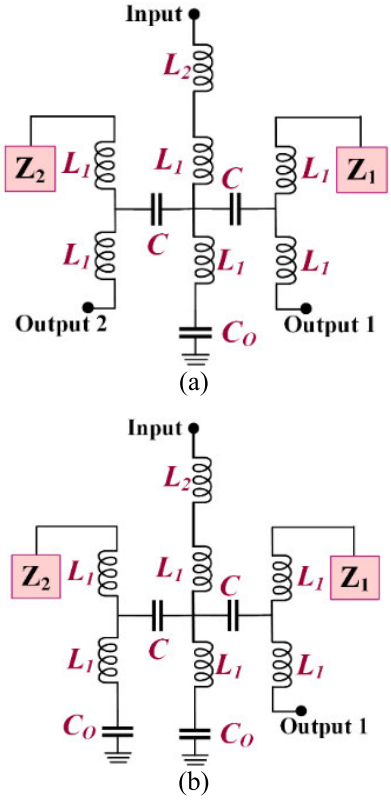

FIGURE 2. Approximated *LC* circuits of the basic (a) three-port structure, (b) bandpass resonator.

coupled lines are depicted by the inductors and capacitors L_1 and C. The capacitor C is related to the coupling effect. The equivalent of a thin line with the physical length l_1 is L_1. In the more exact model, the number of coupling capacitors will be increased and the physical length $2l_1$ will be divided to smaller lines. The open end of middle line is replaced by the capacitor C_O. The transmission line with the physical length l_2 is shown by an inductor of L_2.

In the approximated LC circuits, Z_1 and Z_2 are the impedances of the shunt stubs 1 and 2, respectively. The transfer matrix of the proposed basic bandpass resonator (presented in Fig. 2(b)) will be calculated as follows:

$$M_{T1} = \begin{bmatrix} A_1 & B_1 \\ C_1 & D_1 \end{bmatrix} = \begin{bmatrix} 1 & j\omega(L_1+L_2) \\ 0 & 1 \end{bmatrix} \times \begin{bmatrix} 1 & 0 \\ \frac{1}{Z_3} & 1 \end{bmatrix} \times \begin{bmatrix} 1 & \frac{1}{j\omega C} \\ 0 & 1 \end{bmatrix} \times \begin{bmatrix} 1 & 0 \\ \frac{1}{j\omega L_1 + Z_1} & 1 \end{bmatrix} \times \begin{bmatrix} 1 & j\omega L_1 \\ 0 & 1 \end{bmatrix} \tag{1}$$

ω is an angular frequency and Z_3 is:

$$Z_3 = \frac{[\frac{(j\omega L_1+\frac{1}{j\omega C_O})(j\omega L_1+Z_2)}{j\omega L_1+\frac{1}{j\omega C_O}+j\omega L_1+Z_2)} + \frac{1}{j\omega C}][j\omega L_1 + \frac{1}{j\omega C_O}]}{\frac{(j\omega L_1+\frac{1}{j\omega C_O})(j\omega L_1+Z_2)}{j\omega L_1+\frac{1}{j\omega C_O}+j\omega L_1+Z_2} + \frac{1}{j\omega C} + j\omega L_1 + \frac{1}{j\omega C_O}} \tag{2}$$

The coupling capacitors usually have very small values in fF or pF. Also, the open end capacitor is small. Our target operating frequency is 0.850 GHz and the inductors are in nH. Hence, the following approximations can be used:

$$j\omega L_1 + \frac{1}{j\omega C_O} \approx \frac{1}{j\omega C_O} \tag{3}$$

$$\frac{(j\omega L_1 + \frac{1}{j\omega C_O})(j\omega L_1 + Z_2)}{j\omega L_1 + \frac{1}{j\omega C_O} + j\omega L_1 + Z_2} + \frac{1}{j\omega C}$$
$$\approx \frac{(\frac{1}{j\omega C_O})(j\omega L_1 + Z_2)}{\frac{1}{j\omega C_O}} + \frac{1}{j\omega C} \approx j\omega L_1 + Z_2 + \frac{1}{j\omega C} \approx \frac{1}{j\omega C} \tag{4}$$

$$\frac{(j\omega L_1 + \frac{1}{j\omega C_O})(j\omega L_1 + Z_2)}{j\omega L_1 + \frac{1}{j\omega C_O} + j\omega L_1 + Z_2} + \frac{1}{j\omega C} + j\omega L_1 + \frac{1}{j\omega C_O}$$
$$\approx \frac{1}{j\omega C} + \frac{1}{j\omega C_O} \tag{5}$$

By substituting Equations (3), (4) and (5) in (2):

$$Z_3 \approx \frac{\frac{1}{j\omega C} \times \frac{1}{j\omega C_O}}{\frac{1}{j\omega C} + \frac{1}{j\omega C_O}} = \frac{1}{j\omega(C_O + C)} \tag{6}$$

By substituting Equation (6) in (1), the parameters of transfer matrix M_{T1} can be extracted as follows:

$$A_1 = 1 + \frac{\frac{1}{j\omega C} - \omega^2(C_O + C)(L_1 + L_2)}{j\omega L_1 + Z_1} \tag{7}$$

$$B_1 = j\omega L_1 + [\frac{1}{j\omega C} - \omega^2(C_O + C)(L_1 + L_2)] \times [1 + \frac{j\omega L_1}{j\omega L_1 + Z_1}] \tag{8}$$

$$C_1 = j\omega(C_O + C) + \frac{2 + \frac{C_O}{C}}{j\omega L_1 + Z_1} \tag{9}$$

$$D_1 = -\omega^2 L_1(C_O + C) + [2 + \frac{C_O}{C}] \times [1 + \frac{j\omega L_1}{j\omega L_1 + Z_1}] \tag{10}$$

Based on the values of inductors, capacitors and angular frequency we can use the following approximation to simplify the parameters of M_{T1}:

$$\frac{1}{j\omega C} - \omega^2(C_O + C)(L_1 + L_2) \approx \frac{1}{j\omega C} \tag{11}$$

Therefore:

$$A_1 \approx 1 + \frac{1}{j\omega C(j\omega L_1 + Z_1)} \approx \frac{1}{j\omega C(j\omega L_1 + Z_1)} \tag{12}$$

$$B_1 \approx j\omega L_1 + [\frac{1}{j\omega C}] \times [1 + \frac{j\omega L_1}{j\omega L_1 + Z_1}] \approx [\frac{1}{j\omega C}] \times [1 + \frac{j\omega L_1}{j\omega L_1 + Z_1}] \tag{13}$$

$$C_1 \approx \frac{2 + \frac{C_O}{C}}{j\omega L_1 + Z_1} \tag{14}$$

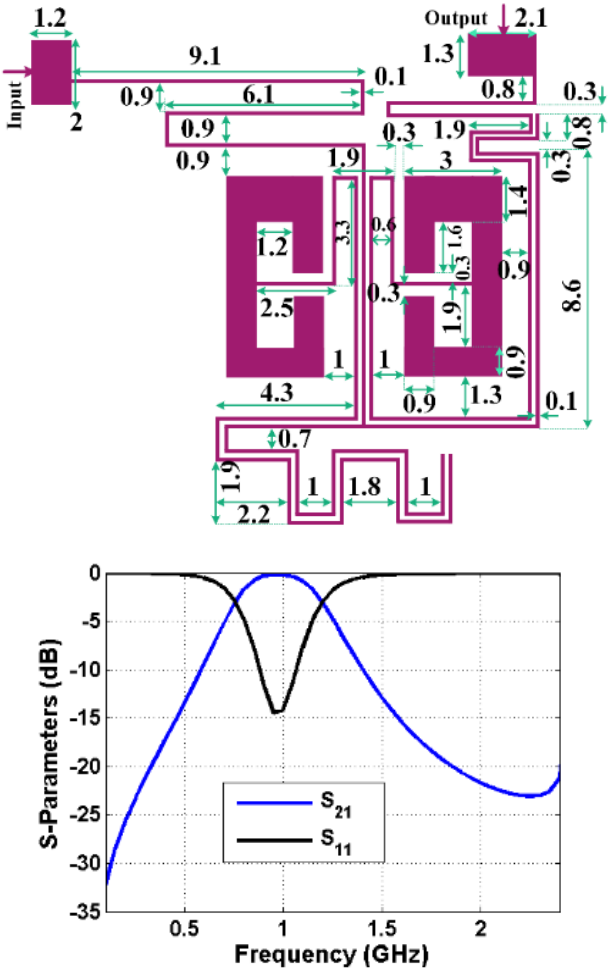

FIGURE 3. BPF1 with its frequency response.

$$D_1 \approx [2 + \frac{C_O}{C}] \times [1 + \frac{j\omega L_1}{j\omega L_1 + Z_1}] \tag{15}$$

The transfer function of the basic bandpass resonator is derived from M_{T1} as follows:

$$H_1(j\omega) = \frac{1}{A_1} \; for \; B_1 = 0 \tag{16}$$

Using Equations (12), (13) and (16) we can write that:

$$H_1(j\omega) = j\omega C(j\omega L_1 + Z_1)$$

and

$$1 + \frac{j\omega L_1}{j\omega L_1 + Z_1} = 0 \rightarrow Z_1 = -2j\omega L_1 \tag{17}$$

According to (17), we can obtain $H_1(j\omega)$ by substituting Z_1 in $H_1(j\omega)$ as follows:

$$H_1(j\omega) = \omega^2 C L_1 \tag{18}$$

The operating angular frequency ω_o will be calculated by setting $H_1(j\omega)$ equal to one:

$$H_1(j\omega_o) = 1 \rightarrow \omega_o \approx \frac{1}{\sqrt{CL_1}} \tag{19}$$

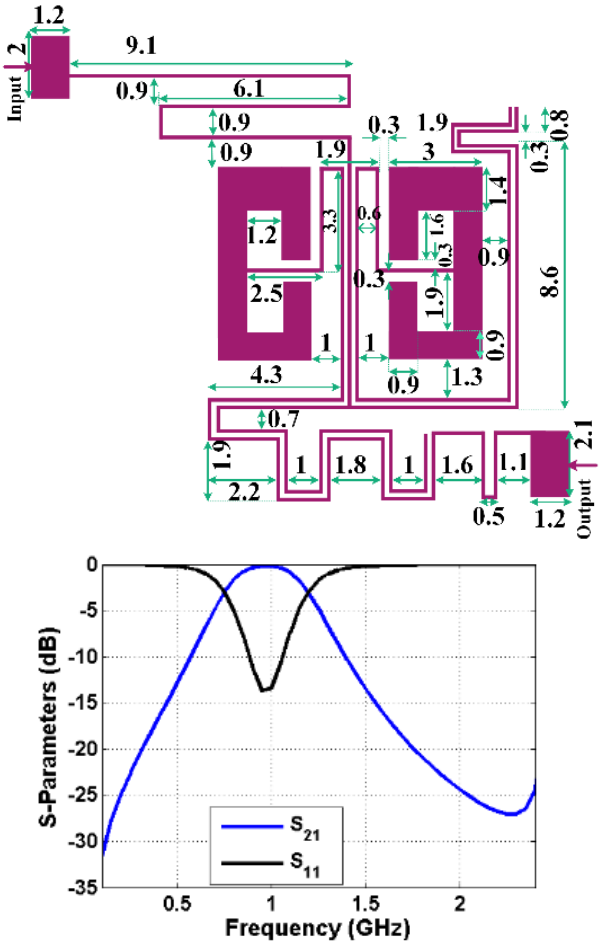

FIGURE 4. BPF2 with its frequency response.

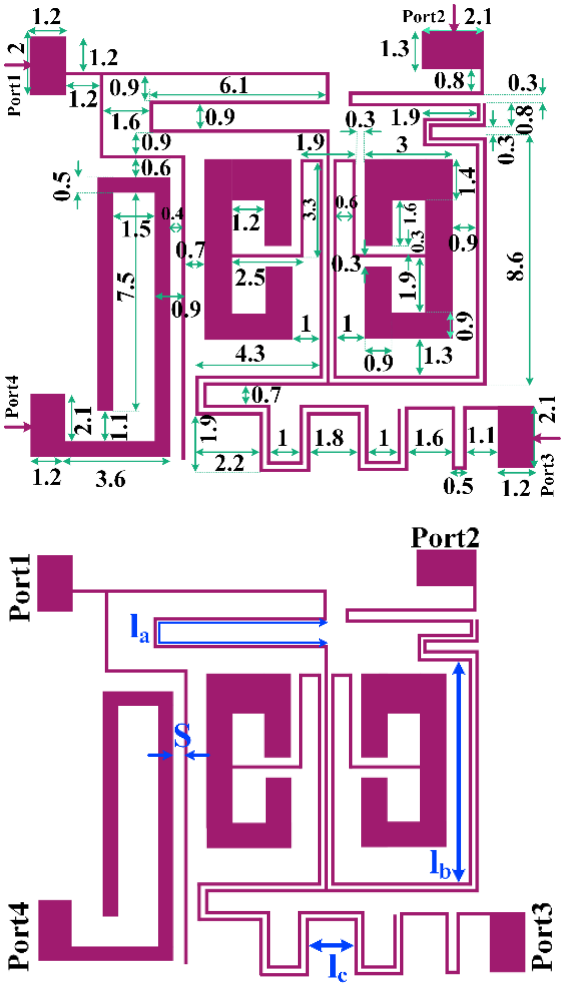

FIGURE 5. Layout configuration of the designed coupler.

Equation (19) demonstrates the ability to tune the coupling capacitor and L_1 for a pre-determined operating frequency. Also, by increasing L_1, the operating frequency moves to the left. Therefore, increasing the physical length $2l_1$ cannot increase the overall size in λg^2 significantly. This shows that the freedom to adjust this physical length is afforded, thereby enabling subsequent adjustment of the operating frequency. To achieve an operating frequency in GHz based on Equation (19), the value of L_1 must be in the nH range when the coupling capacitor is in pF. For example, for a predetermined angular frequency equal to $2\pi \times 0.85$ GHz and $C = 1$ pF from Equation (19) L_1 will be 35 nH.If we set $C = 5$ pF then for $\omega_o = 2\pi \times 0.85$ GHz we have to set $L_1 = 7$ nH.Reducing the space between the coupled lines serves to increase the coupling capacitance. A miniaturized resonator can be achieved under this condition by employing a lower L_1 value. This reduction in L_1 leads to a shorter physical length, $2l_1$.

III. THE PROPOSED COUPLER

Based on the analyzed resonator, two bandpass filters (BPFs) have been designed. These filters are named as BPF1and BPF2. Fig. 3 depicts the BPF1 and its frequency response. As mentioned before, the space between coupled lines is decreased as much as possible to increase the coupling capacitors. The meandering coupled lines are chosen to occupy a small area. The input/output ports are 50 Ω on a Rogers RT/Duroid 5880 substrate (loss tangent = 0.0009, thickness = 0.7874 mm and $\varepsilon_r = 2.22$). This substrate is utilized for the proposed BPFs and coupler. All simulated data in this work are extracted from ADS software using EM simulator. The simulation results show that BPF1 works at 0.95 GHz with a low insertion loss of 0.1 dB. Fig. 4 illustrates BPF2, which is similar to BPF1. However, the outputs locations are different for both filters. It can be seen that both filters have similar frequency responses. The BPF2 works at 0.95 GHz similar to BPF1. It has 0.2 dB insertion loss at its operating frequency.

It can be seen that the frequency responses of the proposed filters are very similar. This is what is needed to create a zero-degree coupler. Using the proposed BPFs, a microstrip coupler is designed as presented in Fig. 5. The dimensions

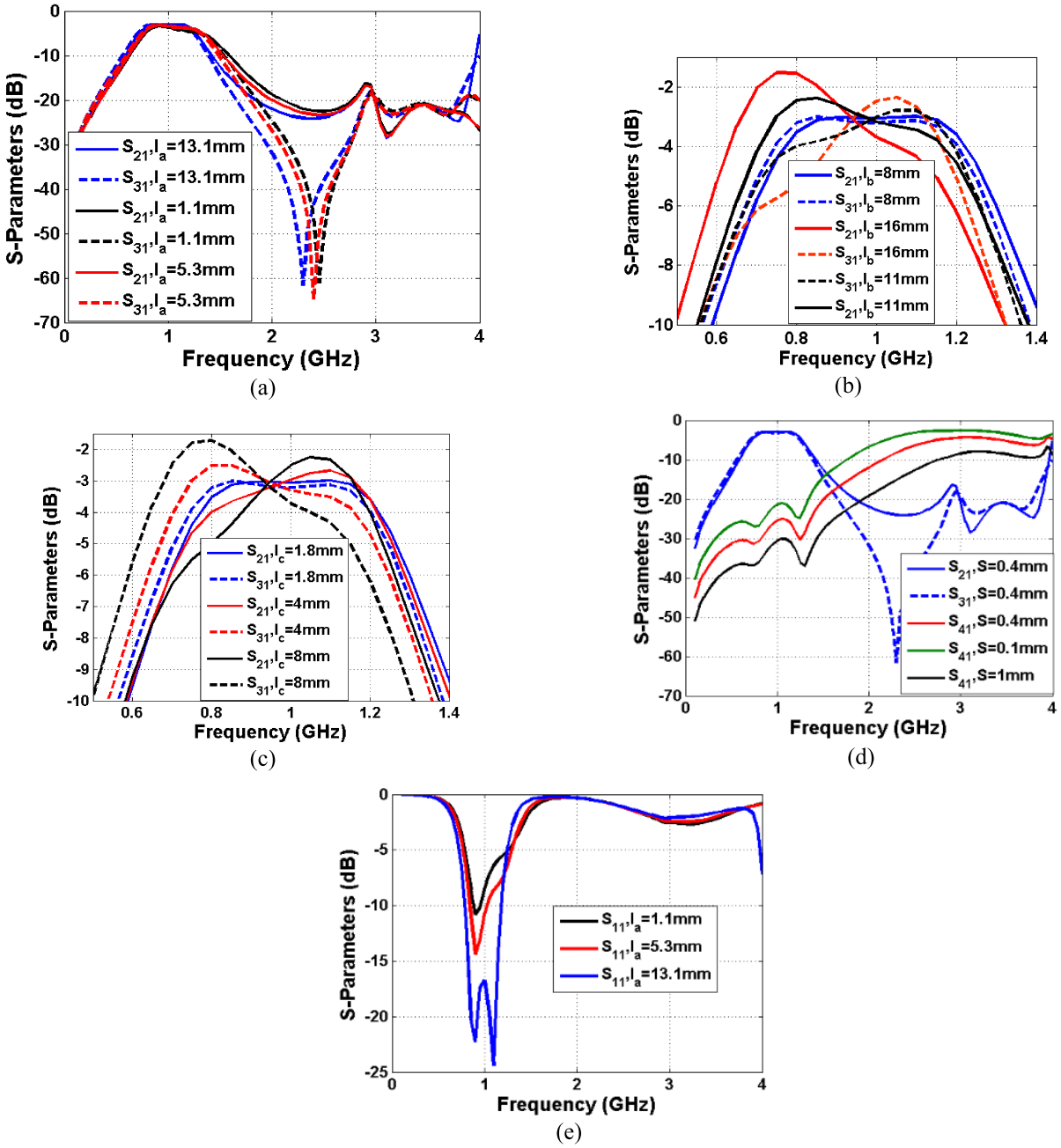

FIGURE 6. S_{21} and S_{31} as the functions of (a) l_a, (b) l_b, (c) l_c, (d) S_{41} as a function of S and (e) S_{11} as a function of la.

of the proposed BPFs in this coupler structure has not been changed. Hence, all dimensions are in mm, the widths of all thin lines are 0.1 mm and the spaces between coupled lines are 0.1 mm. However, the isolation port (Port 4) is coupled to the common port (Port 1), with a space of 0.4 mm between the thinner and wider coupled lines. All tapped line feeding structures have 50 Ω impedances. The overall size of the proposed coupler including I/O ports is 17.3 mm × 15.1 mm (0.06 λg × 0.055 λg). Without I/O ports, the coupler size is 0.0028 λg^2.

The final structure of this coupler is optimized. The scattering parameters as some functions of the effective physical dimensions are depicted in Fig. 6(a)-Fig. 6(e). While the other dimensions are constant, the physical length l_a is changed. The effect of this change on the frequency response is shown in Fig. 6(a). By increasing l_a, the frequency selectivity of S_{31} can be increased. However, increasing this length improves the selectivity. Too much reduction of this physical length will shift the operating frequency to the right. Therefore, the normalized size will be increased. As illustrated in Fig. 6(b)

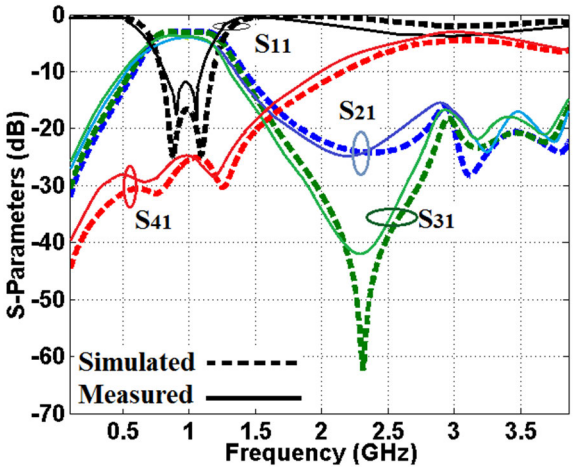

FIGURE 7. S-Parameters of the proposed coupler.

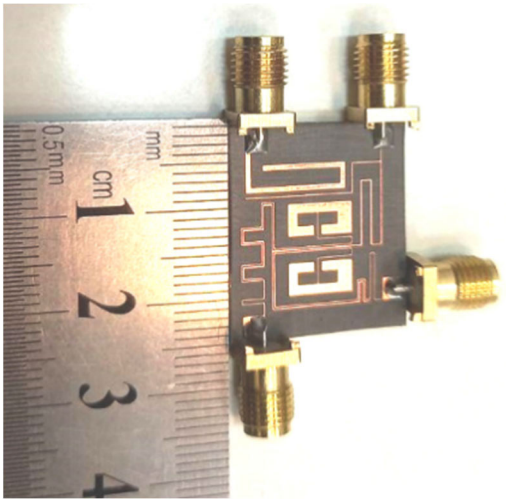

FIGURE 8. Fabricated coupler.

and Fig. 6(c), setting $l_b = 8$ mm and $l_c = 1.8$ mm improves the magnitude balance. Changing S directly affects S_{41}. This is shown in Fig. 6(d). Fig. 6(e) shows that the best value of S_{11} will be obtained for $l_a = 13.1$ mm.

IV. RESULTS AND DISCUSSION

The measured and simulated scattering parameters are demonstrated in Fig. 7, where the measured results are extracted from an HP8757A network analyzer. The simulated and measured balanced magnitude and filtering response can be seen in Fig. 7. However, the simulated losses are a little better than the measured one which is due to copper and SMA losses. As can be seen, it operates at $f_o = 0.875$ GHz. At the operating frequency, the values of S_{11}, S_{21} and S_{31} are -24.97 dB, -3.058 dB and -3.033 dB respectively. Therefore, the magnitude is balanced well. The harmonics are suppressed up to 3.86 GHz ($4.4f_o$) with a maximum level of -16.1 dB. From 0.79 GHz up to 1.18 GHz, the common port return loss is better than -10 dB. Therefore, the fractional bandwidth (FBW) is 40.3%. As shown in Fig. 7, the in-band isolation factor is better than -25 dB. Fig. 8 presents a photograph of our fabricated coupler.

The phase difference of S_{21} and S_{31} is shown in Fig. 9, where the maximum phase unbalance in the bandwidth is better 4.5°. Meanwhile, at the operating frequency the phase of S_{21} and S_{31} are 64.5° and 64°. Therefore, the phase unbalance at the operating frequency is 0.5°. The magnitude difference of S_{21} and S_{31} is shown in Fig. 10, where the maximum magnitude unbalance at the bandwidth is better than ± 0.5 dB. Meanwhile, at the operating frequency the magnitude unbalance is only ± 0.025 dB.

The proposed coupler has been compared with the previous microstrip couplers in Table 1. It can be seen that the most compact size, the best harmonic suppression, the most balanced phases and the lowest magnitude imbalance are obtained in this work. Also, the insertion losses are very low in comparison with the previous couplers. As shown in

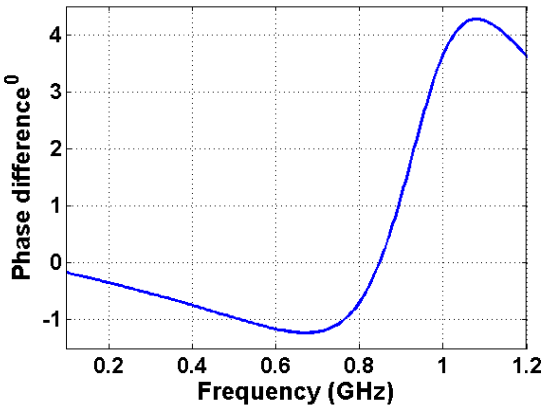

FIGURE 9. Phase difference of S_{21} and S_{31}.

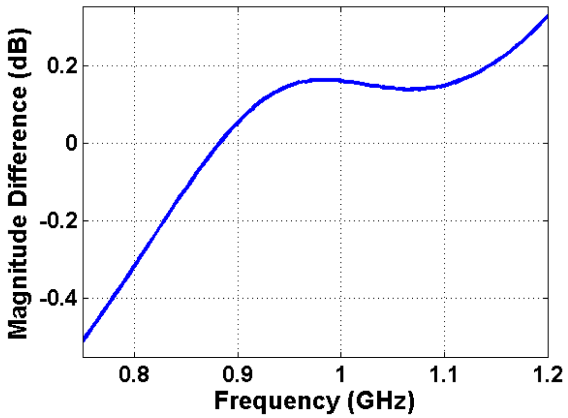

FIGURE 10. Magnitude difference of S_{21} and S_{31}.

Table 1, the designed coupler in [6] has a larger FBW than the proposed one. However, the proposed coupler is smaller and its losses are lower than the presented coupler in [6]. Moreover, the proposed coupler has lower phase shift.

TABLE 1. Performance and size comparison (*: These values are not at operating frequency; PI: Phase Imbalance; MI: Magnitude Imbalance; FR: Filtering Response and SH: Suppressed Harmonic).

Refs	f_o (GHz)	PI°	MI (dB)	$\lvert S_{21}\rvert$/ $\lvert S_{31}\rvert$ (dB)	FR	N^{th} SH	Size (λg^2/ mm^2)	FBW
This coupler	0.875	0.5	0.025	3.058 /3.033	Yes	3rd	0.0028 /204.24	40.3%
[3]	---	---	0.5	----	Yes	No	0.2379 */1157	---
[4]	2	1	0.28	3.11/ 3.39	Yes	2nd	---/265	10%
[6]	2	3	---	---	No	No	--- /1322	56%
[7]	3	2.3	5.13	7.38/ 2.25	No	No	---/819	---
[8]	0.433	2.1	0.32	4.07/ 4.39	No	No	--- /2218	37.8%
[9]	24.52–30	2	0.8	----	Yes	No	0.307* /595	21.1%
[10]	3.5	3.6	0.68	3.65/ 2.97	No	No	0.0432 /448.8	33.4%
[11]	1.87	3	0.5	---	Yes	No	0.138/- --	3.5%
[12]	3.5	10	1	5/3±1	No	No	--- /1553	34.4%

TABLE 2. Group delay of comparison.

References	Type	Maximum Group delay at all channels
This coupler	Coupler	1 ns
[19]	Lowpass-Bandpass Triplexer	2.07 ns
[20]	Lowpass-Bandpass Diplexer	More than 2.5 ns
[21]	Tri-Channel Bandpass Filter	8 ns
[22]	Lowpass-Bandpass Triplexer	6 ns
[23]	Quad-Channel Bandpass Filters	9 ns
[24]	Bandpass-Bandpass Diplexer	Near 4 ns
[25]	Bandpass-Bandpass Diplexer	1.5 ns
[26]	Lowpass-Bandpass Triplexer	1.5 ns

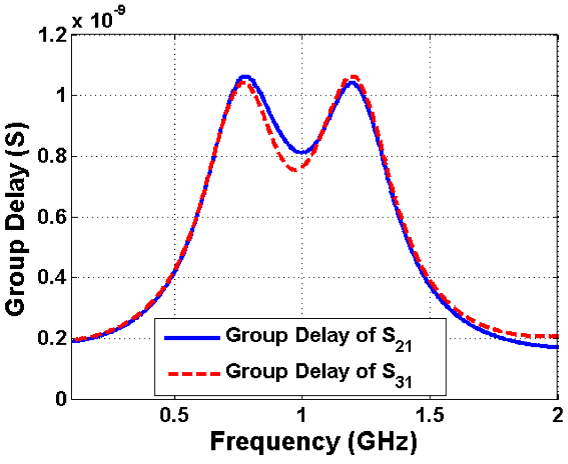

FIGURE 11. Group delays of S_{21} and S_{31}.

The group delay is a significant parameter in the performance evaluation [17], [18]. Hence, the group delays of S_{21} and S_{31} inside the bandwidth are shown in Fig. 11. The maximum group delay of S_{21} is 1.061 ns at 777.5 MHz. Also, the maximum group delay of S_{31} is 1.062 ns at 1.198 GHz. Unfortunately, while this group delay has been investigated, most previous couplers have ignored to highlight this parameter into their account. Therefore, for comparison, the group delay of this proposed coupler has been compared with the group delay of the other passive microstrip devices in Table 2. It is observed that the group delay of the proposed microstrip coupler has a decent value compared to the others.

V. CONCLUSION

A novel microstrip coupler structure based on stub loaded meandrous coupled lines is proposed for modern wireless applications. For obtaining this coupler, first a basic three-port structure consisting of two bandpass filters is proposed and mathematically analyzed to obtain a balanced 0° coupler. The coupler is an ultra-compact device with 0.0028 λg^2 (204.24 mm^2). It has very low insertion losses and two well balanced magnitudes, where at the operating frequency S_{21} and S_{31} are −3.058 dB and −3.033 dB respectively. Another important advantage of this coupler was its filtering response, where it could suppress 1st, 2nd and 3rd harmonics. Meanwhile, it had low group delay, wide bandwidth and flat passbands. The special importance of this coupler is due to having all these advantages at the same time. Meanwhile, the majority of previous works could obtain an advantage by victimizing some of the other factors.

REFERENCES

[1] S. Liu and L. Liu, "A compact directional coupler with high directivity using ferrite cores," *Electron. Lett.*, vol. 59, no. 12, pp. 1–3, Jun. 2023.

[2] C.-H. Chan, T.-C. Yu, and T.-H. Chang, "High-directivity and compact microstrip coupler for RF power applications," *Rev. Sci. Instrum.*, vol. 94, no. 6, pp. 1–18, Jun. 2023.

[3] Y. X. Zhou, L. Xu, F. Wei, and T. Feng, "A wideband balanced filtering coupled-line coupler with improved directivity based on coupled microstrip–slotline," *Microwave Opt. Technol. Lett.*, vol. 66, no. 2, pp. 1–13, Feb. 2024, doi: 10.1002/mop.34049.

[4] J. Wang, B.-Z. Wang, Y.-X. Guo, L. C. Ong, and S. Xiao, "A compact slow-wave microstrip branch-line coupler with high performance," *IEEE Microwave Wireless Compon. Lett.*, vol. 17, no. 7, pp. 501–503, Jul. 2007.

[5] F. Wei, L. Y. Qiao, Y. Han, X.-B. Zhao, L. Xu, R. Li, and X. W. Shi, "A balanced filtering directional coupler based on slotline using asymmetric parallel loaded branches," *IEEE Trans. Compon., Packag., Manuf. Technol.*, vol. 12, no. 7, pp. 1222–1231, Jul. 2022.

[6] Y.-H. Chun and J.-S. Hong, "Compact wide-band branch-line hybrids," *IEEE Trans. Microwave Theory Techn.*, vol. 54, no. 2, pp. 704–709, Feb. 2006.

[7] A. B. Santiko, Y. P. Saputera, and Y. Wahyu, "Design and implementation of three branch line coupler at 3.0 GHz frequency for S-band radar system," in *Proc. 22nd Asia–Pacific Conf. Commun. (APCC)*, Aug. 2016, pp. 315–318.

[8] S. Velan and M. Kanagasabai, "Compact microstrip branch-line coupler with wideband quadrature phase balance," *Microwave Opt. Technol. Lett.*, vol. 58, no. 6, pp. 1369–1374, Jun. 2016.

[9] N. A. Mohd Shukor and N. Seman, "5G planar branch line coupler design based on the analysis of dielectric constant, loss tangent and quality factor at high frequency," *Sci. Rep.*, vol. 10, no. 1, p. 16115, Sep. 2020.

[10] A. A. Abdulbari, S. K. Abdul Rahim, M. Z. Abidin Abd Aziz, K. G. Tan, N. K. Noordin, and M. Z. M. Nor, "New design of wideband microstrip branch line coupler using T-shape and open stub for 5G application," *Int. J. Electr. Comput. Eng. (IJECE)*, vol. 11, no. 2, p. 1346, Apr. 2021.

[11] J. Shi, J. Qiang, K. Xu, Z.-B. Wang, L. Lin, J.-X. Chen, W. Liu, and X. Y. Zhang, "A balanced filtering branch-line coupler," *IEEE Microwave Wireless Compon. Lett.*, vol. 26, no. 2, pp. 119–121, Feb. 2016.

[12] N. A. M. Shukor and N. Seman, "Enhanced design of two-section microstrip-slot branch line coupler with the overlapped λ/4 open circuited lines at ports," *Wireless Pers. Commun.*, vol. 88, no. 3, pp. 467–478, Jun. 2016.
[13] Y. Zhang, X. Tan, and Q. Xiang, "A compact frequency- and power-dividing ratio-tunable quadrature coupler," *Int. J. RF Microwave Comput.-Aided Eng.*, vol. 2023, pp. 1–8, Mar. 2023, doi: 10.1155/2023/8179954.
[14] G. Hu, G. Wang, N. Yang, and Q. Zhang, "Multiobjective optimization design of microstrip directional coupler with generalized coupling slots," *IEEE Trans. Microwave Theory Techn.*, vol. 72, no. 1, pp. 1–10, Jan. 2023, doi: 10.1109/TMTT.2023.3289071.
[15] M. A. Chaudhary, S. Roshani, and S. Roshani, "An ultra compact microstrip branch line coupler with wide stopband using LCL filter and meandered stubs for microwave applications," *Processes*, vol. 11, no. 5, p. 1582, May 2023.
[16] F. H. Ahmed, R. Saad, and S. K. Khamas, "A novel compact broadband quasi-twisted branch line coupler based on a double-layered microstrip line," *Micromachines*, vol. 15, no. 1, p. 142, Jan. 2024.
[17] J. Nako, C. Psychalinos, A. S. Elwakil, and B. J. Maundy, "Power-law negative group delay filters," *Electronics*, vol. 13, no. 3, p. 522, Jan. 2024.
[18] J. Nako, C. Psychalinos, B. J. Maundy, and A. S. Elwakil, "Elementary negative group delay filter functions," *Circuits, Syst., Signal Process.*, vol. 43, no. 6, pp. 3396–3409, Jun. 2024, doi: 10.1007/s00034-024-02647-9.
[19] J. Xu, Z.-Y. Chen, and H. Wan, "Lowpass–bandpass triplexer integrated switch design using common lumped-element triple-resonance resonator technique," *IEEE Trans. Ind. Electron.*, vol. 67, no. 1, pp. 471–479, Jan. 2020.
[20] M. Hayati, A.-R. Zarghami, S. Zarghami, and S. Alirezaee, "Designing a miniaturized microstrip lowpass-bandpass diplexer with wide stopband by examining the effects between filters," *Int. J. Electron. Commun.*, vol. 139, Sep. 2021, Art. no. 153912.
[21] Y. Liu, W.-B. Dou, and Y.-J. Zhao, "A tri-band bandpass filter realized using tri-mode T-shape branches," *Prog. Electromagn. Res.*, vol. 105, pp. 425–444, 2010.
[22] F.-C. Chen, J.-M. Qiu, H.-T. Hu, Q.-X. Chu, and M. J. Lancaster, "Design of microstrip lowpass-bandpass triplexer with high isolation," *IEEE Microwave Wireless Compon. Lett.*, vol. 25, no. 12, pp. 805–807, Dec. 2015.
[23] S.-C. Lin, "Microstrip dual/quad-band filters with coupled lines and quasi-lumped impedance inverters based on parallel-path transmission," *IEEE Trans. Microwave Theory Techn.*, vol. 59, no. 8, pp. 1937–1946, Aug. 2011.
[24] K. Al-Majdi and Y. S. Mezaal, "New miniature narrow band microstrip diplexer for recent wireless communications," *Electronics*, vol. 12, no. 3, p. 716, Feb. 2023.
[25] M. Danaeian, "Miniaturized half-mode substrate integrated waveguide diplexer based on SIR–CSRR unit-cell," *Anal. Integr. Circuits Signal Process.*, vol. 102, no. 3, pp. 555–561, Mar. 2020.
[26] L. Nouri, F. Zubir, L. Nkenyereye, A. Rezaei, M. Abdel-Hafez, F. Hazzazi, M. Akmal Chaudhary, M. Assaad, and Z. B. Yusoff, "Novel ultra-compact wide stopband microstrip lowpass-bandpass triplexer for 5G multi-service wireless networks," *IEEE Access*, vol. 12, pp. 2926–2940, 2024.

SALAH I. YAHYA (Senior Member, IEEE) received the B.Sc. degree in electrical engineering, the M.Sc. degree in electronics and communication engineering, and the Ph.D. degree in communication and microwave engineering. He joined the Department of Software Engineering, Koya University, in 2010, where he is currently a Full Professor. He is also a Consultant Engineer and a Senior Member of USA and AMTA-USA. He has published many research articles in high-quality journals and he presented many conference papers. His research interests include antenna design, numerical RF dosimetry, MW measurement, and MW components design. He has been a regular Reviewer of Electromagnetics Academy, Cambridge, USA, PIERS journals publications, *Science and Engineering of Composite Materials* journal, and *International Journal of Applied Electromagnetics and Mechanics*, since 2009.

FARID ZUBIR (Member, IEEE) received the B.Eng. degree in electrical (telecommunication) and the M.Eng. degree in RF and microwave from Universiti Teknologi Malaysia (UTM), in 2008 and 2010, respectively, and the Ph.D. degree from the University of Birmingham, U.K., in 2016, for research into direct integration of power amplifiers with antennas in microwave transmitters. He is currently an Assistant Professor and a Research Fellow with the Department of Communication Engineering, School of Electrical Engineering, and the Wireless Communication Centre, UTM. He was an Honorary Postdoctoral Research Fellow with The University of British Columbia (UBCO), Okanagan, BC, Canada, from September 2019 to August 2021, where he conducted research into highly efficient and linear amplification power amplifier topology for wireless power systems. His research interests include the area of RF and microwave technologies, including linearization and high-efficiency techniques for PAs, beamforming networks, planar array antenna, dielectric resonator antenna (DRA), and active integrated antenna (AIA).

LEILA NOURI received the B.Sc. and M.Sc. degrees in electronic engineering from Razi University, Kermanshah, Iran, in 2005 and 2009, respectively, and the Ph.D. degree in electronic engineering from the Shiraz University of Technology. She is the author of one book, more than 70 articles, and more than five research and industrial projects. Her research interests include microstrip couplers, microstrip filters, neural networks, and LNAs.

ABBAS REZAEI, photograph and biography not available at the time of publication.

NOORLINDAWATY MD JIZAT (Member, IEEE) received the B.E. and M.S. degrees in electrical engineering (telecommunication) from Universiti Teknologi Malaysia (UTM), in 2008 and 2010, respectively. She is currently pursuing the Ph.D. degree in electrical engineering (telecommunication) with Multimedia University (MMU), Malaysia. From 2008 to 2012, she was a Quality Engineer with Flextronics Technology Sdn Bhd and a Research and Development Engineer with Panasonic System Network Malaysia. She is a Lecturer with the Faculty of Engineering, MMU. Her research interests include beamforming networks, butler matrices, beam steering, antenna arrays, self-powered solar Wi-Fi systems, and material research into antenna applications.